Cukurova University
Journal of
Natural & Applied Sciences

Original Paper

Optimization of post curing in mask stereolithography

Ana Pilipović[1], Leonarda Vukonić[1]

[1]University of Zagreb, Faculty of Mechanical Engineering and Naval Architecture; Croatia

ORCID IDs of the authors: A.P. 0000-0003-1330-6458; L.V. 0000-0002-4405-6204.

Cite this article as: Pilipović, A., Vukonić, L. (2022). Optimization of post curing in mask stereolithography, Cukurova University Journal of Natural & Applied Sciences 1 (1): 31-40.

Abstract

Additive production (also called 3D printing) allows the production of products of complicated geometry in a short produc-tion time. Even after 35 years of development since the initial prototyping, to this day some procedures are still exclusively for prototyping. Mask stereolithography (MSLA) is a low-budget process that uses liquid for production in which there are many processing parameters that could affect the improvement of mechanical properties and thus allow the application of the process for making functional products. The processes have many advantages, but one of the biggest disadvantages is the need for post curing after processing. In this paper, the effect of post curing time on tensile properties was determined. After that, the optimization of the post curing process was performed, which shows that the desirability function within the range of post curing time is only 0.566, which does not fully meet the set criteria of maximum values of tensile properties, especially tensile strain.

Keywords: Analysis of variance, mask stereolithography, optimization, post curing, tensile properties.

Nomenclature: CLIP – continuous liquid interphase printing, DF – degree of freedom, LCD – liquid-crystal display, LED – light emitting diode, DLP – digital light processing, MSLA – mask stereolitography, SLA – stereolitography, UV – ultraviolet, d – desirability, h [mm] – thickness, E [N/mm^2] – tensile modulus, r^2 – R-squared, SSD - sum of square deflection, t_{pc} [min] – post curing time, σ_m [N/mm^2] – tensile strength, ε_b [%] – tensile strain at break.

1. Introduction

In the last ten years, there has been an intensive development of additive production processes. As an advanced technology, it is used today to produce parts of relatively complicated geometry, with high speed and precision. According to the standard ISO/ASTM 52900: 2015, additive manufacturing are divided into 7 categories: vat photopolymerization, material jetting, binder jetting, material extrusion, powder bed fusion, sheet lamination and direct energy deposition. One of the earliest developed category of additive manufacturing process is the vat photopolymerization, in which the material is cured by the action of light radiation.

Photopolymerization is a special type of condensation polymerization based on the crosslinking of liquid monomers / oligomers using a light source of a certain wavelength to form crosslinked resins. In order for crosslinking of polymers, photoinitiators are necessary, which initiate a photochemical reaction, ie convert photolytic energy into free radicals and reactive oxygen species. Free radicals and reactive oxygen species then stimulate chain growth, or crosslinking. Depending on the mechanism of the photochemical reaction, photopolymerization can be radical or cationic. [1]

Radical photopolymerization takes place under light radiation, when a photoinitiator or photoinitiator system converts photolytic energy into free radicals and thus initiates the photopolymerization process. Typical groups of polymers in which photopolymeri-

Address for Correspondence:
Ana Pilipović, e-mail: ana.pilipovic@fsb.hr

Received: January 14, 2022
Accepted: February 17, 2022

zation takes place by a radical mechanism are: methacrylates and polymers with thiol-en or thiol-in reactions. Cationic photopolymerization takes place with the help of cationic photoinitiators made of aryl-iodinated salts or sulfonium photoinitiators, which initiate photopolymerization under ultraviolet (UV) radiation, ie form reactive groups. The reactivity of the photoinitiator depends on the structure of the monomer applied. The source of light radiation can be xenon lamps, light bulbs, light emitting diode (LED) lamps or lasers. Wavelengths range between the UV (190-400 nm) region, the visible light region (400-700 nm) and the infrared region (700-1000 nm). [1] Electromagnetic curing is most commonly used; UV radiation and visible light radiation. [2]

Photopolymerization processes can be divided according to the source of electromagnetic radiation (Figure 1) on stereolithography (SLA), digital light processing (DLP), mask stereolithography (MSLA), continuous liquid interphase printing (CLIP).

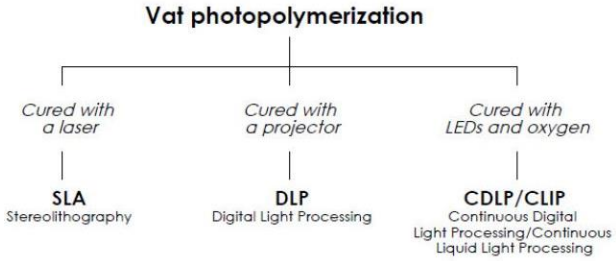

Figure 1. Classification of vat photopolymerization processes [2]

In all vat polymerization processes when heat is applied to an object, molecules and atoms vibrate faster which causes the space between them to increase. The application of heat in the photopolymer curing process allows for improvement in the strength and stiffness of an object through an increase in molecule mobility within the polymer network. Curing of photopolymers relies on highly reactive free radicals bonding with open reactive groups within the polymer network. Heat applied to an object during post-curing will increase the mobility of free radicals within the polymer network and increase the likelihood that a reactive free radical will find an unreacted double bond within the network rather than reacting with another free radical which would result in a neutral effect to mechanical properties of the object [3].

The degree of cure is a function of different parameters that can be related to the resin composition or manufacture parameters. Usually, green parts (after being built by the VP process) can reach at least an 80% degree of cure, since a fully cured part is not easy to obtain. A post-cure procedure is then necessary, and the use of a UV chamber or thermal oven may increase curing up to 90%. For parts built with urethane acrylic-based resins, the result may be low strength and cure shrinkage. Therefore, it is essential to understand the operating parameters, which influence the degree of cure of the liquid photosensitive resin [4].

2. Mask stereolithography (MSLA)

The MSLA process uses an liquid-crystal display (LCD) screen to project an image [5]. The LCD screen consists of a number of pixels, each of which is composed of two polarizing filters between which are liquid crystal molecules. The filter lines are positioned relative to each other at a 90° angle, and the light source is located behind the first filter. Liquid crystal molecules can be rotated if there is potential between the filters, but between the filter plates they are arranged so that without the presence of the potential difference between the plates, the light beam rotates 90°, with the rays passing through the second filter [6].

Plates with transparent electrodes touch the liquid crystal and orient its molecules in certain directions. The light transmission is controlled by the applied voltage to the electrodes, since the magnitude of the applied voltage determines how much the liquid crystal molecules will rotate and thus affect the polarization angle of the filter [6].

Figure 2. MSLA 3D printer

The MSLA printer (Figure 2) consists of a light source (LED projector), a work surface and a chamber. The LCD screen is actually part of the light source itself. 10% of the light, which has an approximate wavelength between 350 nm and 420 nm, is transmitted only through unlit pixels, and in these places the photosensitive material is cross-linked, while the remaining 90% is absorbed by the LCD screen. Since the pixel size of the LCD screen is set at the factory and cannot be changed depending on the size of the product, the resolution depends significantly on the volume of the product itself. The LED light also cannot be corrected without the use of lenses. As with the DLP process, the whole layer hardens at once, so compared to the SLA process, the production is much faster. At the end of the illumination of the first layer, the work surface is raised / lowered (depending on whether is the bottom-up or -down performance of the 3D printer) to a level outside the photosensitive liquid in order to remove the tension of the surface between the liquid and the work surface itself. The next layer is illuminated and the procedure is repeated until the last layer is finished [5, 7, 8].

The materials used in the MSLA process are, as in the DLP process, radical photosensitive resins, since the same light source is used. However, as the method of projection, and thus the light intensity, is different, in order to use exactly the same types of resins, it is necessary to increase the amount of photoinitiator or extend the exposure time. The MSLA procedure is applied in the fields of dental medicine, jewelry making, toys and others [5].

The advantages are: curing of the whole layer at once, significantly faster process compared to SLA, cheap device, higher resolution for the same product than in the DLP process [5, 9].

Disadvantages are: low light intensity, short life of the LCD screen, the need for cleaning after each production, the required support structure [5, 9].

3. Experimental Part

3.1 Production of the test specimens

The test specimen were made on a 3D printer *Anycubic Photon* according to the standard HRN EN ISO 527-2: 2012 type 1BA with a thickness of h = 4 mm. Processing parameters are specified in the *Chitubox* software, and they are: layer height 0.1 mm, exposure time 15 s, light-off delay 1 s, lifting speed 65 mm/min, bottom layer count 3, bottom exposure time 60 s, bottom light-off delay 1 s, bottom lift distance 5 mm, bottom lift speed 35 mm/min, retract speed 150 mm/min and anycubic white material with UV light wavelength of 405 nm.

Three test specimens were made for each experiment, and they were made in one cycle according to Figure 3.a (test specimens were made at an angle of 20° in relation to the x and y axis with a supporting structure). The 3D printing time was 2h and 28 min. After fabrication, the test specimen were placed in isopropanol for 30 s and washed with water. After that, the test specimens, according to the experiment plan, were post cured in a UV chamber with a rotating table (Figure 3.b) [10].

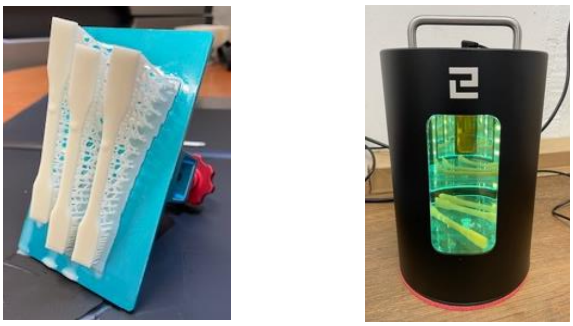

a) b)

Figure 3. Test specimens: a) after production on a 3D printer *Anycubic Photon*, b) in UV chamber for post curing [10]

3.2 Analysis method

The experiment plan was done in the software *Design Expert* using ANOVA response surface - one factor design. The upper limit of the post curing time was determined due to the increasing color change of the product up to a maximum of 9 min. Table 1 shows 8 experimental states with factor A (post curing time t_{pc}) and tensile properties results. Three test specimens were tested for each experimental condition on the universal testing machine *Shimadzu AGS-X* with max. force 10 kN. The mean values and standard deviation were then calculated and shown in Table 1. The tensile strength was equal to the tensile stress at break in all test specimens.

Table 1. Design plan and results of the tensile properties

Std	Factor A: post curing time t_{pc}, min	Tensile strength σ_m, N/mm^2	Tensile strain at break ε_b, %	Tensile modulus E, N/mm^2
1	4.30	38.468 ± 2.33	5.016 ± 0.31	1041.06 ± 48.74
2	0	26.375 ± 3.58	11.779 ± 0.19	501.009 ± 107.29
3	4.30	37.797 ± 2.85	5.451 ± 1.20	1011.16 ± 107.71
4	0	26.097 ± 1.05	14.577 ± 4.60	494.14 ± 140.61
5	2.25	30.612 ± 1.43	4.264 ± 0.67	829.106 ± 34.86
6	9	41.773 ± 1.33	5.341 ± 0.54	1095.14 ± 68.47
7	6.25	39.634 ± 1.78	5.452 ± 0.66	1049.00 ± 164.71
8	9	38.328 ± 6.44	4.556 ± 1.30	1095.74 ± 86.56

Figure 4 shows the tensile stress-strain curves of the mean values of all 8 experimental states.

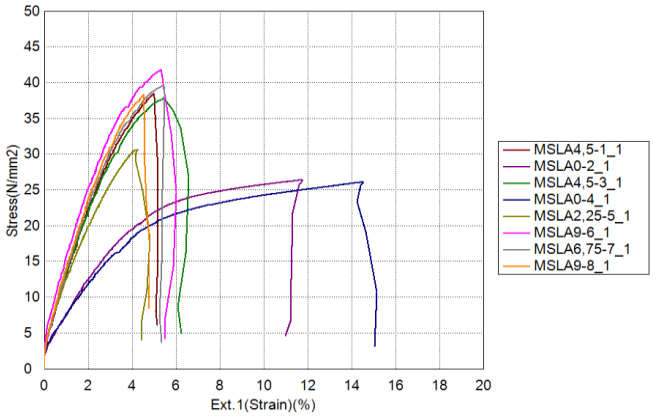

Figure 4. Tensile stress – strain diagram (curves of 8 std of the mean values)

3.3 Results

Table 2 gives the analysis results, and Table 3 shows the basic statistical data for the model of tensile strength from software *Design Expert*.

Table 2. Results of the variance analysis for the tensile strength

Source	Sum of squares	DF	Mean square	F value	Prob > F
Model	259.01	2	129.51	53.61	0.0004 significant
A	229.55	1	229.55	95.02	0.0002
A^2	29.46	1	29.46	12.20	0.0174
Residual	12.08	5	2.42		
Lack of fit	5.90	2	2.95	1.43	0.3685 non significant
Pure error	6.18	3	2.06		
Cor total	271.09	7			

For a certain factor to affect the change, the Prob > F value should be smaller than 0.05 [11]. In the case of interpretation of the tensile strength results, a square model was chosen. It can be concluded from the table that factor A and A^2 have a significant influence on the change of the tensile strength. Likewise, the deviation from the model (lack of fit) was non significant, which meant that the selected model was appropriate.

Table 3. Overview of the statistical data about the model for the tensile strength

	Tensile strength σ_m, MPa
Standard deviation	1.55
Mean	34.88
Coefficient of determination r^2 (*R*-squared)	0.9554

R-squared (r^2) is the measure of deviation from the arithmetic mean, which is explained by the model. The closer r^2 is to 1, the model better follows the data. The calculation of R-squared is made according to Equation [11]:

$$r^2 = 1 - \frac{SSD_{residual}}{SSD_{model} + SSD_{residual}} \quad (1)$$

where r^2 is the R-squared and *SSD* is the sum of square deflection.

From Table 3, it can be concluded that the model followed the data very well since the coefficient of determination was $r^2 = 0.954$.

With regression analysis a mathematical model for calculating tensile strength σ_m as a function of post curing time t_{cp} was obtained:

$$\sigma_m = 25.862 + 3.498 \cdot t_{pc} - 0.212 \cdot {t_{pc}}^2 \quad (2)$$

The dependency of the post curing time on the tensile strength is shown in Figure 5.

It can be seen in the figure that as the post curing time increases, the tensile strength increases sharply, and asymptotically approaches the value of about 40 MPa.

Table 4 gives the analysis results, and table 5 shows the basic statistical data for the model of tensile strain at break from software *Design Expert*.

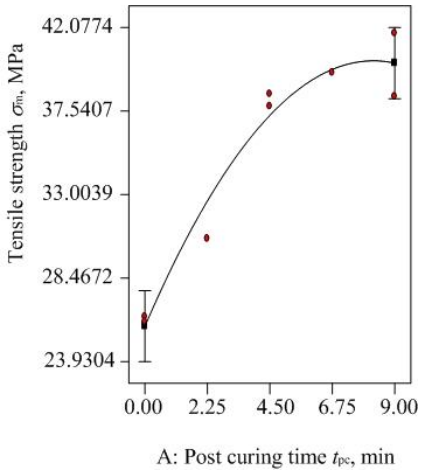

Figure 5. Dependence of the post curing time on the tensile strength

Table 4. Results of the variance analysis for the tensile strain at break

Source	Sum of squares	DF	Mean square	F value	Prob > F
Model	98.66	3	32.89	20.05	0.0071 significant
A	2.44	1	2.44	1.49	0.2894
A^2	30.22	1	30.22	18.42	0.0127
A^3	12.51	1	12.51	7.63	0.0508
Residual	6.56	4	1.64		
Lack of fit	2.24	1	2.24	1.56	0.3002 non significant
Pure error	4.32	3	1.44		
Cor total	105.22	7			

In the case of interpretation of the tensile strain at break results, a cubic model was chosen. It can be concluded from the table that factor A^2 have a significant influence on the change of the tensile strain at break. The deviation from the model (lack of fit) was non significant, which meant that the selected model was appropriate. This occured only with the cubic model.

Table 5. Overview of the statistical data about the model for the tensile strain at break

	Tensile strain at break ε_b, %
Standard deviation	1.28
Mean	7.06
Coefficient of determination r^2 (*R*-squared)	0.9376

From Table 5, it can be concluded that the model followed the data very well since the coefficient of determination was r^2 = 0.9376.

With regression analysis a mathematical model for calculating tensile strain at break ε_b as a function of post curing time t_{cp} was obtained:

$$\varepsilon_b = 13.0751 - 5.99349 \cdot t_{pc} + 1.26294 \cdot {t_{pc}}^2 - 0.077622 \cdot {t_{pc}}^3 \quad (3)$$

The dependency of the post curing time on the tensile strain at break is shown in Figure 6.

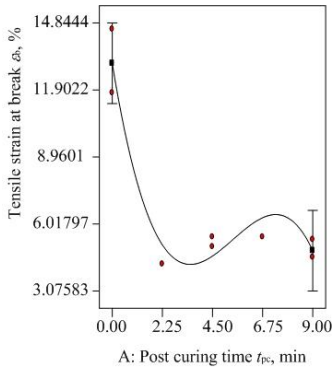

Figure 6. Dependence of the post curing time on the tensile strain at break

It can be seen in Figure 6 that the post curing time sharply reduces the strain to a value between 4-5.5%.

Table 6 gives the analysis results, and Table 7 shows the basic statistical data for the model of tensile modulus from software *Design Expert*.

Table 6. Results of the variance analysis for the tensile modulus

Source	Sum of squares	DF	Mean square	F value	Prob > F
Model	$4.573 \cdot 10^5$	3	$1.524 \cdot 10^5$	387.37	< 0.0001 significant
A	10453.5	1	10453.5	26.56	0.0067
A^2	75724.75	1	75724.75	192.41	0.0002
A^3	2776.94	1	2776.94	7.06	0.0566
Residual	1574.21	4	393.55		
Lack of fit	1103.49	1	1103.49	7.03	0.0769 non significant
Pure error	470.71	3	156.9		
Cor total	$4.589 \cdot 10^5$	7			

In the case of interpretation of the tensile modulus results, a cubic model was chosen. It can be concluded from the table that factor A and A^2 have a significant influence on the change of the tensile modulus. The deviation from the model (lack of fit) was non significant, which meant that the selected model was appropriate. This occured only with the cubic model.

Table 7. Overview of the statistical data about the model for the tensile modulus

	Tensile modulus *E*, MPa
Standard deviation	19.84
Mean	889.54
Coefficient of determination r^2 (*R*-squared)	0.9966

From Table 7, it can be concluded that the model followed the data very well since the coefficient of determination was r^2 = 0.9966.

With regression analysis a mathematical model for calculating tensile modulus E as a function of post curing time t_{cp} was obtained:

$$E = 495.24422 + 210.14974 \cdot t_{pc} - 26.37808 \cdot {t_{pc}}^2 + 1.15658 \cdot {t_{pc}}^3 \quad (4)$$

The dependency of the post curing time on the tensile modulus is shown in Figure 7.

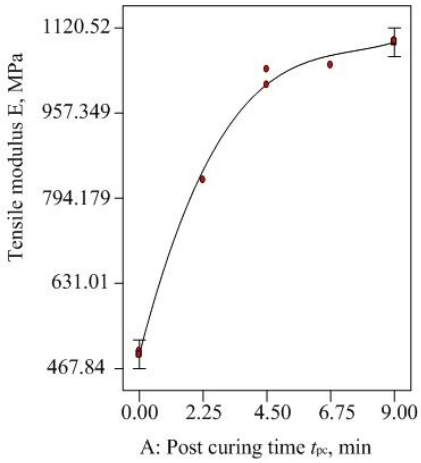

Figure 7. Dependence of the post curing time on the tensile modulus

In Figure 7 it can be seen that as the post curing time increases, the tensile modulus rises sharply where at a maximum post curing time of 9 min, the value of the modulus is 1100 MPa.

3.4 Optimization

Software package Design Expert also includes an optimization module, in which optimization can be performed based on the desirability functions. The optimization process searches for a combination of factor values that simultaneously satisfy the criteria (wishes and priorities) placed on each of the responses and factors [11]. For best results the desirability function must be close to 1. In this research, optimization was performed with optimization criteria (for optimal solution): maximum tensile strength, tensile strain at break and tensile modulus with post curing time in experiment range (0-9 min). Optimization constraints and criteria are given in Table 8.

Table 8. Constraints and optimization solution

Name	Goal	Lower limit	Upper limit	Solution 1	Solution 2
Post curing time t_{pc}, min	in range	0	9	7.43	1.52
Tensile strength σ_m, N/mm^2	maximum	26.1	41.77	40.1327	30.6861
Tensile strain at break ε_b, %	maximum	4.26	14.58	6.42499	6.6123
Tensile modulus E, N/mm^2	maximum	494.14	1095.74	1074.9	757.687

For the given optimization conditions, only two solution was found, which is given in Table 8. Desirability for solution 1 is d = 0.566 and for solution 2 desirability d = 0.308 resulting that optimization did not completely satisfy the set criteria. In solution 1 the maximum tensile strength and modulus condition is satisfied, while the tensile strain at break is not, so it could be expected that the desirability function would be slightly worse. The post curing time dependence on the tensile properties within the optimization constraints is shown in Figure 8.

4. Discussion

In their works, the authors Slade, D. [3] and Zguris, Z. [12] made an identical experiment with resins crosslinking at 405 nm wavelength and concluded that first there is a sudden jump in the increase in strength and modulus, but only after 30 min of post curing, these values are kept at approximately the same amount. However, it is interesting that the temperature of the post curing has a greater role in increasing the strength and modulus, so that the test specimens achieve higher strength and modulus with the higher temperature of the post curing.

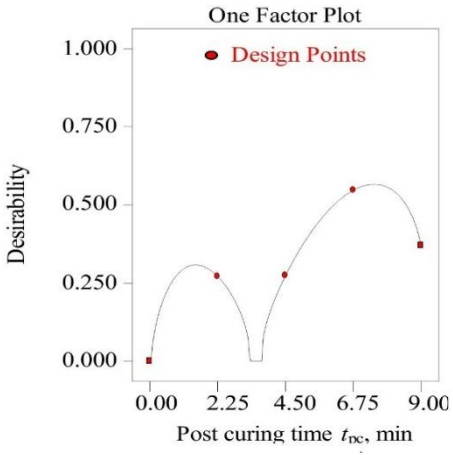

Figure 8. Desirability of the post curing time on the tensile properties

Another work from authors Kim et al. [13] shown that strength increased when it was post cured for 60-90 min and also that increased in post curing time shows the greater color change which is also the conclusion of this paper. However, the results obtained by our experiment are obtained after post curing time of 9 min, which in these works takes much more time 60-90 min and 120 min. They also did not test elongation, which decreases significantly with increasing other values of tensile properties, up to 64% of the initial value. Work of Reymus et al. [14] concluded that post curing depends on the thickness of the printed layer in such a way that the layer thickness of 0.1 and 0.05 mm has a higher conversion than when the layer thickness is 0.025 mm. In this paper, a constant layer thickness of 0.1 mm was taken, and this certainly opens the need for further research. Wu et al. [15] investigate how UV post curing in DLP printing process can lead to shape distortion and thus reduction of dimension accuracy. It was found that the distortion of a DLP printed object depends on both the gradient of addition degree of conversion in the material during the post-curing process as well as the stiffness of the structure. From the test results it can be seen that the strength and modulus increase while the tensile strain decreases. Strain decreases from the initial value of 14% to 4-5.5% regardless of the duration of post curing, which can be seen on the curve in Figure 6. It is very important to mention that the time of post curing also affects the color of the final product, due to which, when planning the production process, it is necessary to determine which final properties are to be achieved, ie which properties are of crucial importance for the final application of the product. If the color of the final product is one of the priority requirements, according to the test and analysis it can be concluded that the time of post curing in the UV chamber is limited to a maximum of 6 minutes, since by that time the color change is negligible. From the optimization it was concluded that in the post curing time to 9 min it is not possible to meet the criterion that all tensile properties are maximum.

5. Conclusion

Additive production is a process that is moving forward more and more every day, new materials and new processes are being developed. However, all these procedures for the time being entail some types of post-processing, as examined in this paper. The influence of the time of POST CURING on the tensile properties and color change was determined experimentally and it was found that there is no need in the MSLA procedure post curing higher than 6 min, which is significantly less than in the ster-olithography.

Acknowledgement

This work is a part of research included in the project *Increasing Excellence on Advanced Additive Manufacturing - INEX-ADAM* financed from the European Union's Horizon 2020 research and innovation programme under grant agreement No 810708. The authors would like to thank the European Union for funding.

References

[1] Bagheri, A. and Jin, J. (2019). Photopolymerization in 3D Printing, ACS Applied Polymer Materials, 1 (4), pp.593-611.

[2] Pagac, M., Hajnys, J., Ma, Q.-P., Jancar, L., Jansa, J., Stefek, P. and Mesicek, J. (2021). A Review of Vat Photopolymerization Technology: Materials, Applications, Challenges, and Future Trends of 3D Printing, Polymers, 13, 598.

[3] Slade, D. Effects of print and post-cure parameters on mechanical properties of 3D printed parts, New-Pro3D, https://wiki.ubc.ca/images/f/ff/EFFECTS_OF_PRINT_AND_POST-CURE_PARAMETERS_ON_MECHANICAL_PROPERTIES_OF_3D_PRINTED_PARTS.pdf, consulted 12 August 2021.

[4] Salmoria, G.V., Ahrens, C.H., Beal, V.E., Pires, A.T.N. and Soldi V. (2009). Evaluation of post-curing and laser manufacturing parameters on the properties of SOMOS 7110 photosensitive resin used in stereolithography, Materials and Design 30 758–763, doi:10.1016/j.matdes.2008.05.016

[5] Quan, H., Zhang, T., Xu, H., Luo, S., Nie, J. and Zhu, X. (2020). Photo-curing 3D printing techniques and its challenges, Bioactive Materials, 5(1): 110-5. DOI: 10.1016/j.bioactmat.2019.12.003

[6] https://electronics.howstuffworks.com/lcd.htm#pt4, consulted 25 May 2021.

[7] https://www.structo3d.com/pages/mask-stereolithography-msla-technology, consulted 25 May 2021.

[8] Mao, Y., Miyazaki, T., Sakai, K., Gong, J., Zhu, M. and Ito, H. (2018). A 3D printable Thermal Energy Storage Crystalline Gel Using Mask-Projection Stereolitography, Polymers, 1-14, 10, 1117. DOI: 10.3390/polym10101117

[9] https://diyodemag.com/education/exploring_3d_masked_stereolithography_3d_printing 25.05.2021, consulted 25 May 2021

[10] Vukonić, L. Influence of post curing in masked stereolithography, diploma thesis, University of Zagreb, FSB, Zagreb, 2021.

[11] Rujnić-Sokele, M (2007). Influence of the stretch blow moulding processing parameters on PET bottles properties, Polimeri, 284, pp.213–292.

[12] Zguris, Z. How Mechanical Properties of Stereolithography 3D Prints are Affected by UV Curing, Formlabs, https://archive-media.formlabs.com/upload/How-Mechanical-Properties-of-SLA-3D-Prints-Are-Affected-by-UV-Curing.pdf, consulted 12 August 2021.

[13] Kim, D., Shim, J., Lee, D., Shin, S., Nam, N., Park, K., Shim, J., Kim, J. (2020). Efects of Post-Curing Time on the Mechanical and Color Properties of Three-Dimensional Printed Crown and Bridge Materials, Polymers 2020, 12, 2762; doi:10.3390/polym12112762

[14] Reymus, M., Lümkemann, N., Stawarczyk, B (2019). 3D-printed material for temporary restorations: impact of print layer thickness and post-curing method on degree of conversion, Int J Comput Dent. 2019; 22(3):231-237.

[15] Wu, D., Zhao, Z., Zhang, Q., Qi, H.J., Fang, D. (2019). Mechanics of shape distortion of DLP 3D printed structures during UV post – curing, Soft Matter, 2019,15, 6151-6159.